Biharmonic Friction with a Smagorinsky-Like Viscosity for Use in Large-Scale Eddy-Permitting Ocean Models

Stephen M. Griffies and Robert W. Hallberg

NOAA Geophysical Fluid Dynamics Laboratory, Princeton, New Jersey

(Manuscript received 26 July 1999, in final form 14 January 2000)

ABSTRACT

This paper discusses a numerical closure, motivated from the ideas of Smagorinsky, for use with a biharmonic operator. The result is a highly scale-selective, state-dependent friction operator for use in eddy-permitting geophysical fluid models. This friction should prove most useful for large-scale ocean models in which there are multiple regimes of geostrophic turbulence. Examples are provided from primitive equation geopotential and isopycnal-coordinate ocean models.

1. Introduction

A key goal of large-scale ocean modeling where mesoscale eddies are permitted is to achieve simulations in which the natural tendency for oceanic flows to exhibit hydrodynamic instabilities and turbulence is not handicapped by overly strong frictional dissipation. That is, the desire is to allow dynamics at the resolved scales of motion to dominate the subgrid-scale parameterization. Such simulations impose fewer a priori assumptions on the flow associated with details of the subgrid-scale operator. Ideally, the result is a simulation that more faithfully represents the rich variety of observed oceanic flow regimes.

In practice, it is impossible to completely remove friction from a numerical simulation. In particular, ocean models require frictional dissipation in order to suppress instabilities such as those associated with the grid Reynolds number, to provide a vorticity sink at western boundaries, and to generally suppress power at unresolved scales. Indeed, in the presence of geostrophic turbulence, friction must be sufficient to absorb enstrophy upon cascading toward the smallest resolved scales. Finally, frictional dissipation can be included as a physical parameterization of the effect of unresolved scales on the resolved scales. Currently, however, there is no generally agreed upon form of a physically motivated closure for linear momentum in ocean models. Notably, Laplacian momentum friction *has not* been motivated

from first principles at the scales resolved in large-scale ocean models.

Consequently, one can identify the two central roles of friction: numerical closure and physical parameterization. It is not uncommon for the friction to be described as though it were a physical parameterization of small scales, even though the chosen value of viscosity may be set by numerical stability considerations. However, these two very distinct considerations should be thought of separately in designing dissipation schemes for ocean models.

The focus here is on the numerical closure aspects of friction. Yet our inspiration stems from the ideas of Smagorinsky (1963, 1993), who was motivated from physically based turbulence closure arguments. The key point made in this paper is that the Smagorinsky approach, when combined with a biharmonic operator, is ideal for global ocean modeling in the presence of mesoscale variability. This combination provides an extremely effective device for use in maintaining numerical stability, without adversely affecting the resolved scales of flow.

Since the inertial range of a geostrophic turbulence cascade conserves total energy, it is desirable to have the frictional operator remove a minimal amount of kinetic energy from the scales of physical interest. That is, we wish friction to keep the flow within the bounds of numerical stability requirements without adversely affecting the resolved part of the spectrum where energy is concentrated. If set to a strength sufficient to suppress numerical instabilities, the Laplacian form of friction significantly removes both kinetic energy and enstrophy over a broad range of spatial scales. For this reason, more highly scale-selective frictional operators, such as biharmonic or higher-order operators, are often used for

Corresponding author address: Dr. Stephen M. Griffies, NOAA Geophysical Fluid Dynamics Laboratory, P.O. Box 308, Forrestal Campus, Princeton, NJ 08542.
E-mail: smg@gfdl.gov

quasigeostrophic simulations (e.g., Holland 1978; Held et al. 1995) as well as primitive equation models (e.g., Semtner and Mintz 1977; Böning and Budich 1992). The anticipated potential vorticity approach of Sadourny and Basdevant (1985) goes one step further by formally conserving energy while dissipating enstrophy.

When using a biharmonic operator, the predominant practice in ocean modeling is to also employ a state-independent biharmonic viscosity. To maintain numerical stability, this coefficient must be set large enough to control the most vigorous anticipated motions. Such a choice may be suitable for simulations with one regime of flow, although it will lead to more dissipation than is numerically required when the flow exhibits temporal and spatial variability. When simulating realistic ocean flows that contain multiple space–time varying flow regimes and employ variable grid resolutions, such dissipation will generally be excessive in many important regions. The discussion by Gille (1997) illustrates this point in an analysis of the Southern Ocean momentum budget with an eddy-permitting global ocean simulation.

Smagorinsky (1963, 1993) proposed that the effective Laplacian viscosity due to unresolved scales should be proportional to the resolved horizontal deformation rate times the squared grid spacing. This scheme is a physically plausible parameterization of the effects of three-dimensional isotropic turbulence, and it has found much use in large-eddy simulations (e.g., see Galperin and Orszag 1993 for a compendium). For large-scale geophysical fluid simulations, however, it has little physical justification since the unresolved scales are dominated by quasi-two-dimensional geostrophic turbulence. For this reason, Leith (1968, 1996) proposed an alternative approach based on two-dimensional turbulence. Leith's viscosity is proportional to the horizontal gradient of the relative vorticity times the cubed grid spacing. This approach has found some use in atmospheric models (e.g., Boer and Shepherd 1983), but it is not commonly used in ocean models.

The Smagorinsky scheme has found notable use in large-scale ocean models (e.g., Blumberg and Mellor 1987; Rosati and Miyakoda 1988; Bleck and Boudra 1981; Bleck et al. 1992) for pragmatic reasons. First, it is more convenient to compute than the Leith viscosity due to the smaller required grid stencil, and because the deformation rate used to compute the Smagorinsky viscosity is furthermore needed to compute the stress tensor. Second, as with the Leith scheme, the Smagorinsky viscosity tailors the local dissipation to both the local flow state and local grid resolution with only a single, nondimensional adjustable parameter. If this parameter is properly chosen, the resulting viscosity ensures that the flow respects the relevant numerical stability properties, even when simulating multiple flow and grid regimes such as occur in realistic ocean simulations.

Although the use of a Smagorinsky viscosity with a Laplacian frictional operator is less dissipative than a constant viscosity, we have found that the Laplacian form of the operator remains overzealous in its dissipation of large-scale energy. As illustrated in sections 4 and 5, the result can be overdissipation of the eddies and, hence, a suboptimal use of the model's resolved scales. For this reason, we propose the use of a Smagorinsky-like viscosity with a biharmonic operator as an appropriate numerical closure scheme for eddy-permitting ocean models. A similar idea was mentioned by Bleck and Boudra (1981) and Sadourny and Maynard (1997). In this approach, the biharmonic viscosity is proportional to the resolved deformation rate times the grid spacing to the fourth power, $|D|\Delta^4$, rather than $|D|\Delta^2$ as used with the Laplacian operator. This *biharmonic Smagorinsky scheme* retains the enhanced scale selectivity of a biharmonic viscosity, as well as the pragmatic aspects of the Smagorinsky scheme mentioned above.

Even without resolved eddies, the proposed biharmonic Smagorinsky scheme will be a useful numerical closure when combined with a physically based parameterization of unresolved turbulence. Consequently, observations and/or theory can be used to specify the form and magnitude of the physical parameterization, rather than also having to be concerned with numerical stability constraints. To the extent that the physical parameterization is less scale selective than the biharmonic operator, the dominant dissipative effect on the well-resolved scales will be associated with physics, not numerics. A recent illustration of this approach is given in the paper by Kazantsev et al. (1998), in which a constant viscosity Laplacian operator provided their numerical closure, and statistical mechanics provided their physical closure.

The organization of this paper is the following. Section 2 reviews the scale selectivity and numerical stability properties of the Laplacian and biharmonic operators in support of the previous discussion. Section 3 introduces the Smagorinsky Laplacian and biharmonic viscosities and discusses their properties according to the numerical stability constraints of section 2. Section 4 presents an eddy-permitting channel experiment using the Modular Ocean Model (MOM), which is a three-dimensional, geopotential-coordinate, primitive equation, B-grid ocean model (Pacanowski and Griffies 1999). This example serves to illustrate the overdissipation resulting from Laplacian friction relative to the biharmonic friction, even when using a Smagorinsky viscosity. Section 5 presents an example of an eddy-permitting midlatitude wind-driven sector experiment using the Hallberg isopycnal model (HIM), which is a three-dimensional, isopycnal-coordinate, primitive equation, C-grid ocean model (Hallberg 1995). This example illustrates the utility of the Smagorinsky approach in a model with meridional boundaries and hence a very inhomogeneous flow field. Section 6 provides a summary and conclusions. An appendix documents the Laplacian and biharmonic friction operators valid in any set of horizontal orthogonal coordinates and nonorthogonal vertical coordinates. We also present here a dis-

cussion of the discretization choices made when implementing these ideas on the Arakawa B and C grids.

2. Scale selectivity and numerical stability

The purpose of this section is to summarize the basic ideas regarding the scale selectivity of the biharmonic friction relative to the Laplacian friction, as well as to discuss some of the numerical stability considerations that constrain the size of the viscosity. Much of the discussion here is limited to the case of constant viscosity and a uniform grid. However, the ideas correspond locally to cases with a nonconstant viscosity used on a nonuniform grid.

a. Scale selectivity of the frictional operators

Although standard, it is nonetheless useful to begin our discussion with a simple illustration of the enhanced scale selectivity of the biharmonic operator over the Laplacian. For this purpose, we proceed much as Semtner and Mintz (1977) and Holland (1978) by considering the following linear equations in one Cartesian dimension using constant viscosities

$$\psi_t = A\psi_{xx} \quad \text{and} \tag{1}$$

$$\psi_t = -B\psi_{xxxx}, \tag{2}$$

with $A > 0$ the Laplacian viscosity, $B > 0$ the biharmonic viscosity, and ψ a model field, such as velocity. The evolution of a monochromatic grid wave $\psi = c(t)e^{ikx_n}$ (where k is a wavenumber, $x_n = n\Delta$ are the grid points, and Δ is the uniform grid spacing) takes the form of a damped exponential. Using centered differences in space, the spindown times

$$\tau_L = A^{-1}\left[\frac{2}{\Delta}\sin(k\Delta/2)\right]^{-2} \quad \text{and} \tag{3}$$

$$\tau_B = B^{-1}\left[\frac{2}{\Delta}\sin(k\Delta/2)\right]^{-4} \tag{4}$$

have a ratio τ_L/τ_B that falls off in a roughly quadratic fashion as the wavenumber decreases and reaches a maximum at the highest resolved wavenumber $k = \pi/\Delta$. Consequently, the longer waves, which are also better resolved, have longer spindown times with the biharmonic operator, given the same spindown time for the shorter waves. The wavenumber where the two operators exhibit the same spindown times depends on the values chosen for the viscosities. As discussed below, for reasons of diffusive stability we are motivated to consider $B = A(\Delta^2/8)$ when relating the Smagorinsky Laplacian and biharmonic viscosities. With this choice, for example, grid-scale waves, with $k = \pi/\Delta$, are damped twice as fast with the Laplacian operator than with the biharmonic operator, whereas 10Δ waves, with $k = \pi/(10\Delta)$, are damped 80 times faster, and 20Δ waves

are damped 320 times faster. This behavior illustrates what is meant by *scale selectivity*—the biharmonic operator more strongly selects the small scales to dissipate and leaves the large scales relatively untouched.

b. Scale selectivity versus adaptive dissipation

Since the Smagorinsky viscosity is based on the local deformation rate, it can be tuned to provide the minimum dissipation consistent with numerical stability. However, we wish to distinguish this *adaptive dissipation* property from that of the enhanced scale selectivity of a biharmonic operator. For this purpose, consider the one-dimensional case in which the Smagorinsky viscosity takes the form $A = (C\Delta/\pi)^2|u_x|$, with C an empirically chosen constant, and so the diffusion equation for momentum is given by

$$u_t = [(C\Delta/\pi)^2|u_x|u_x]_x. \tag{5}$$

For a monochromatic wave $u = c(t)\exp(ikx_n)$, the resulting k^3 on the right-hand side may suggest a more scale-selective operator than in the constant viscosity case. Indeed, it is more scale selective when the flow is *completely* described by a single wave. However, for a realistic flow in which there are many scales, the scale of the largest shear, which sets the viscosity, can be associated with a wavenumber k^*. Once this scale is set, the right-hand side scales as k^2 for the other waves, just as for a constant viscosity. That is, scale selectivity, which is a property of the frictional operator, is distinct from an ability to adaptively reduce dissipation through use of a spatially dependent viscosity

As a specific example, we have evaluated the dissipation associated with three superimposed waves, with relative wavenumbers 3, 4, and 25, and relative amplitudes 1, ½, and ½. The Smagorinsky viscosity varies quite rapidly, due to the wavenumber 25 wave, but it has a mean value that is a substantial fraction of its maximum value. The dissipation of the wavenumber 3 and 4 waves is within 1% of the dissipation that would be provided by the mean viscosity. In particular, the ratios of the spindown rates of the wavenumber 3 and 4 waves are almost exactly $(¾)^2$.

c. Stability of the diffusion equation

Sufficient conditions for numerical stability of the linear equations (1) and (2) can be found using a von Neumann analysis (e.g., Haltiner and Williams 1980). For centered differences in space and forward differences in time, one finds for one spatial dimension, $A < \Delta^2/(2\Delta t)$, whereas for two dimensions,

$$A < \frac{\Delta^2}{4\Delta t}, \tag{6}$$

where $\Delta^2 = 2[(\Delta x)^{-2} + (\Delta y)^{-2}]^{-1}$. Note that use of $\Delta = \min(\Delta x, \Delta y)$ is conservative and is used in the fol-

lowing. For the biharmonic operator in two dimensions, a sufficient condition for stability is

$$B < \frac{\Delta^2}{8} A_{\max}, \tag{7}$$

where $A_{\max} = \Delta^2/(4\Delta t)$.

For global ocean models, the convergence of the meridians can make this constraint more limiting on the available time steps than the Courant–Freidrichs–Lewy (CFL) constraint. This situation occurs especially when one attempts to use a globally constant viscosity relevant for resolving the western boundary layer in the midlatitudes. A common practice to overcome this constraint is to taper the viscosity according to the grid spacing (e.g., Smith et al. 2000). The local grid dependence of the Smagorinsky viscosity naturally accounts for the convergence of the meridians, as well as other nonuniform grid configurations such as enhanced equatorial resolution.

d. Grid Reynolds number constraint

Instead of considering the balance between time tendency and friction, consider now a steady-state balance between advection and Laplacian friction

$$U\psi_x = A\psi_{xx}, \tag{8}$$

where U is a constant advection velocity. Using centered differences in space, Bryan et al. (1975) showed that the finite-difference counterpart of this equation will suppress a computational mode if

$$\frac{U\Delta}{A} < 2. \tag{9}$$

That is, the Reynolds number[1] based on the grid scale must be less than two. Similar considerations for the balance $U\psi_x = -B\psi_{xxxx}$ leads to $U\Delta^3/B < \alpha$, where α is generally tedious to determine, yet with $\alpha = 16$ motivated by combining the constraints (7) and (9).

In coarse-resolution models, not satisfying the grid Reynolds number constraint typically ensures a noisy solution. In the presence of an eddying flow, independent of the discretization choice, a viscosity satisfying a similar constraint is necessary to prevent velocity self-advection from steepening velocity gradients into grid-scale velocity shocks, as described in one dimension by Burgers's equation $u_t + uu_x = Au_{xx}$. Failure to do so can result in an unbounded solution.

e. The frictional boundary layer

Horizontal friction is a leading-order term near western boundaries and, thus, creates a frictional boundary layer (e.g., Munk 1950; Gill 1982). With Laplacian fric-

---

[1] Also called the grid Peclet number when ψ is a tracer.

tion, the Munk boundary layer L_{bdy} has a width proportional to $(A/\beta)^{1/3}$, where β is the planetary vorticity gradient. For biharmonic friction, the boundary layer width is set by $L_{\text{bdy}} \propto (B/\beta)^{1/5}$.

Experience has shown that if the boundary layer is not resolved by the model grid, that is, if $\Delta x > L_{\text{bdy}}$, then the model's circulation will be noisy (e.g., Bryan et al. 1975). Physically, the problem is related to not applying a sufficient level of vorticity dissipation from which the western boundary current can deposit the torque input from external forcing throughout the basin. A common practice is to allow at least two grid points within the Munk layer. Indeed, for MOM, the work of Griffies et al. (2000) argued for the necessity of doing so in order to reduce the amount of spurious diapycnal mixing arising from errors in numerical tracer advection.

With increasing model resolution, the western boundary layer constraint becomes less of a limiting factor than the Reynolds number constraint. The ratio of the viscosities necessary to satisfy the two constraints takes the form $A_{\text{Re}}/A_{\text{bdy}} = U\Delta/(2L_{\text{bdy}}^3\beta) \propto U/(2\Delta^2\beta)$. For biharmonic viscosity, $B_{\text{Re}}/B_{\text{bdy}} \propto U/(16\Delta^2\beta)$. The advective velocity scale U typically increases with decreasing grid spacing, thus guaranteeing that the viscosity ratios are increasing functions of resolution. Hence, the boundary layer constraint is more important in regimes where the flow is sluggish, such as occurs in coarse-resolution models, whereas the Reynolds constraint is more important for vigorous flows, such as those in fine-resolution models.

f. Comments on tracer diffusivity

At scales relevant for large-scale ocean models, it is physically unclear how the momentum viscosity and tracer diffusivity should be related. The numerical constraints determining the magnitude of the diffusivity are analogous to those for viscosity, except that there is no corresponding frictional boundary layer constraint. Typically, we have found it sufficient, for numerical closure, to set the diffusivity to a time-independent constant that is a function only of the grid spacing and that is generally much smaller than the viscosity in the frictional boundary regions. Issues of physical closure for the tracer equation are topics of intense research, and are not the subject of this paper.

3. The Smagorinsky viscosity

A length scale and timescale are sufficient to determine a kinematic viscosity. For the timescale, Smagorinsky (1963, 1993) chose the deformation rate

$$T^{-1} = |D| = \sqrt{D_T^2 + D_S^2}. \tag{10}$$

In Cartesian coordinates, the horizontal tension $D_T = u_x - v_y$, and the horizontal shearing strain $D_S = u_y + v_x$. Generalizations to arbitrary coordinates, as well as

further discussion, are given in the appendix. For the length scale, Smagorinsky chose the maximum wavenumber admitted by the horizontal grid

$$L^{-1} = \pi/\Delta. \tag{11}$$

For generally anisotropic grids, we choose to set $\Delta \equiv \min(\Delta x, \Delta y)$. The resulting viscosity is given by

$$A_{smag} = (C\Delta/\pi)^2|D|, \tag{12}$$

where C is a dimensionless scaling parameter. Smagorinsky, and various other researchers, have provided physically based arguments for specifying the value of C (see in particular Smagorinsky 1993 and references therein). For our purposes, it is empirically determined based on details of the numerical model.

The central idea in this paper is to generalize the above to a biharmonic viscosity by simply multiplying the Smagorinsky Laplacian viscosity by $\Delta^2/8$, leading to

$$B_{smag} = A_{smag}\Delta^2/8. \tag{13}$$

The factor of 1/8 arises from considerations of linear stability given by Eq. (7).

Given these expressions for the Smagorinsky viscosity, it is useful to summarize how it obeys the three numerical stability considerations just described. It is sufficient to consider the case of a Laplacian operator in one spatial dimension. The three constraints can be summarized as

$$A_{smag} > U\Delta/2, \tag{14}$$

$$A_{smag} > \beta\Delta^3, \quad \text{and} \tag{15}$$

$$A_{smag} < \Delta^2/(2\Delta t). \tag{16}$$

If the deformation rate scales as U/Δ, the Smagorinsky viscosity then has the scale

$$A_{smag} = (C/\pi)^2 U\Delta. \tag{17}$$

The grid Reynolds number constraint (14) then implies that the Smagorinsky dimensionless scaling coefficient must satisfy $C > \pi/\sqrt{2} \approx 2.2$. Taking the minimum value yields the Smagorinsky viscosity $A_{smag} = U\Delta/2$, which satisfies the linear diffusion equation constraint (16) provided that the advection velocity satisfies the advective CFL constraint $U\Delta t/\Delta < 1$. Note that ocean models are often more stringently constrained by Doppler-shifted gravity wave speeds $U_g > U$. In our applications, we have found values of $C \approx 3$–4 to be suitable. Note that these values are larger than those suggested by Smagorinsky (1993) based on arguments from three-dimensional turbulence.

The constraints (14) and (15) suggest three distinct regimes for large-scale ocean models. When resolution is coarse and flows are weak, the need to resolve western boundary currents is the most stringent constraint on the level of viscosity. In this regime, we have found the Laplacian Smagorinsky scheme, using a minimum allowable viscosity set by the Munk boundary layer constraint, to be of use. In general, such a minimum set by

frictional boundary layer constraints is necessary in the more quiet deeper ocean, where both the Laplacian and biharmonic Smagorinsky viscosities can be insufficient to resolve boundary currents. With more vigorous flows allowed with higher resolutions, but resolutions that are still too coarse to permit a well-represented geostrophic energy/enstrophy cascade, the Reynolds number constraint becomes more important than the western boundary layer constraint. In this case the biharmonic Smagorinsky scheme is an ideal numerical closure when combined with a physically based parameterization of the effects of the unresolved scales. With a Smagorinsky biharmonic scheme satisfying both the Reynolds number and western boundary constraints, the physically based viscosity can be set by theory or observations, rather than numerics. The third regime is one in which the resolution is sufficiently high, compared to the deformation radius, that the enstrophy cascade to small scales is well represented. In this case, the Smagorinsky biharmonic scheme alone is suitable.

4. A thermally forced channel model

This section illustrates how the use of a Laplacian friction operator, even with a Smagorinsky viscosity, can overdamp otherwise physically unstable and numerically well-resolved waves. The configuration we employ is a zonally reentrant, flat-bottom channel configuration using the primitive equation, geopotential-coordinate ocean model MOM (Pacanowski and Griffies 1999). The experiment is initialized from rest with a stratification achieved by running a coarse-resolution version for 4000 yr, at which time the vertical stratification is stationary and there is a large store of available potential energy. Thereafter, the solution is interpolated to a higher horizontal grid resolution, and a small amount of grid noise is added in order to initiate the growth of baroclinically unstable modes. A similar model configuration and experimental procedure has been used by Griffies et al. (2000). Further details are given in the caption to Fig. 1.

Shown in Fig. 1 are snapshots of the temperature field at 300 m and day 400. The left panel in Fig. 1 is the result when using the biharmonic Smagorinsky scheme, and the right panel in Fig. 1 uses a Laplacian Smagorinsky scheme. Each simulation used a Smagorinsky scaling coefficient $C = 2$. Day 400 occurs in the middle of the growing phase of the most unstable wave. By day 800, each solution has reached a peak in kinetic energy.

As suggested by the analysis in section 2a, we see that the Laplacian operator heavily dissipates the growing waves. Indeed, there is relatively little nonlinear wave activity for the Laplacian solution, whereas the biharmonic solution has reached a stage of strong nonlinear turbulent mixing. By day 800, the biharmonic solution has 18 times more kinetic energy than the Laplacian solution, and it has almost completed the fa-
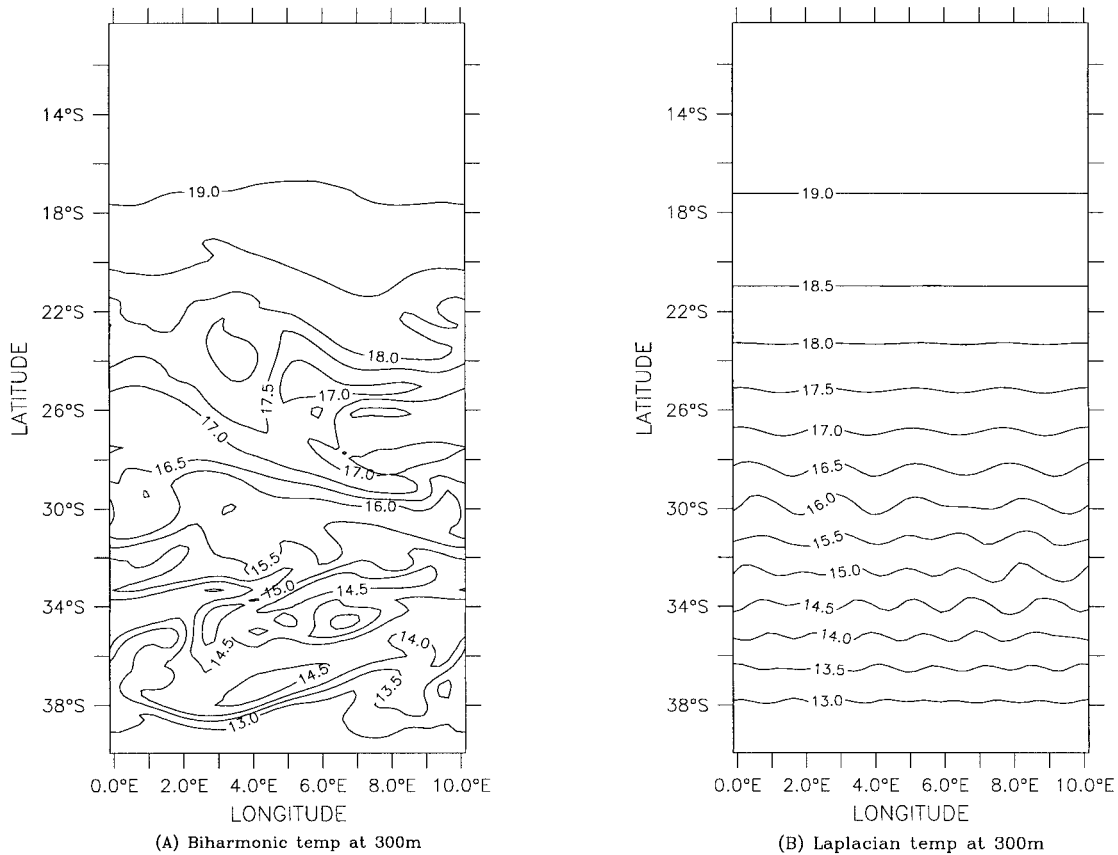
FIG. 1. Results from a zonally reentrant channel configuration using MOM. The domain extends from 10° to 40°S, and is 10° in longitude. The horizontal grid is locally square, so that the latitudinal resolution $\Delta\phi$ is given by $\Delta\lambda \cos\phi$, where $\Delta\lambda$ = ¼. The vertical resolution is a uniform 25 m from the surface to the bottom at 1200 m. The vertical viscosity is a constant 10^{-4} m^2 s^{-1}, and the vertical diffusivity is a constant 2×10^{-5} m^2 s^{-1}. The quicker advection scheme (Leonard 1979; Holland et al. 1998) is used for advecting temperature. A thermal restoring force of 28 W m^{-2} (°C)$^{-1}$ provides the only external forcing. There is no bottom friction. The horizontal Prandtl number is unity. The equation of state is linear. Each panel shows results at 300-m depth (level 12) after 400 days of integration. (left) Temperature using biharmonic Smagorinsky. (right) Temperature using Laplacian Smagorinsky.

miliar quasigeostrophic turbulence process of nonlinear transfer from the baroclinic modes to the barotropic mode (e.g., Rhines 1977; Salmon 1998).

Other experiments with the Laplacian operator were conducted to further investigate what was necessary to allow for a stronger growth of the unstable waves. To do so, we ran cases with much smaller values of the Smagorinsky scaling coefficient (as small as $C = 0.5$), as well as with various levels of constant horizontal viscosity. Consistently, for those cases that did generate nontrivial turbulence, the Laplacian solution was underdissipated and, so, was characterized by a substantial amount of power at the grid scale.

We conclude from this experiment that the analysis presented in section 2a has a great deal of relevance to the ability of a model to admit geostrophic turbulence through the growth of baroclinically unstable waves. The use of Laplacian friction, even when employing a Smagorinsky viscosity, suppresses the growth of the unstable waves. It either yields trivial levels of turbulence,

or fails to dissipate the enstrophy cascade as it reaches the grid scale. Only by moving toward much higher grid resolution will the dissipation levels at the relevant wavelengths be small enough for the Laplacian friction to admit turbulence in this model, while still absorbing the associated enstrophy cascade.

For the current experiment, the biharmonic friction required roughly 10% more total computational time on a Cray T90 processor than the case with the Laplacian. This cost should be compared to that engendered by adding the higher grid resolution needed to permit an analogous level of turbulence with the Laplacian operator.

5. A wind-driven sector model

We now follow up the thermally forced channel simulations with wind-driven sector experiments using the primitive equation, isopycnal ocean model HIM (Hallberg 1995). Notably, the presence of meridional bound-

aries introduces strong inhomogeneities that are always present in realistic ocean simulations. These inhomogeneities provide the key difference from the channel experiments.

There are no diapycnal mass fluxes in these simulations, so the mean stratification in each simulation is identical. The western boundary current spawns a vigorous eddy field, even with a Laplacian viscosity. The wind forcing has a strength typical for the North Atlantic, and the Ekman pumping pattern drives a familiar two-gyre circulation. All of these simulations are run to 10 000 days, with a statistically steady state attained at about 4000 days. The resolution of $\frac{1}{6}° \times \frac{1}{5}°$ (a square grid of 18.5 km at 33.5°N) is adequate for representing the first baroclinic deformation radius of about 40 km. The vertical resolution of five isopycnal layers permits the development of baroclinic eddies with a reasonable vertical gyre structure.

The Smagorinsky biharmonic viscosity exhibits strong spatial variations (Fig. 2). The flow deformation rate (and hence the viscosity) is intense near the surface in the western boundary current region and around the separated western boundary current. Strong eddies are shed from the separated western boundary current, and these give rise to a broad region of enhanced time mean viscosity. In the eastern portion of the basin, and especially in the abyssal shadow region (Luyten et al. 1983), the viscosity is substantially smaller. In this simulation, there is a variation of over two orders of magnitude in the viscosity between the most and least energetic regions. In each region, the viscosity is adequate to maintain numerical integrity (i.e., satisfy the grid Reynolds number and frictional boundary layer constraints) without causing more dissipation than is necessary.

The same simulation was repeated with a constant biharmonic viscosity replacing the Smagorinsky viscosity. To determine the constant viscosity, we tried taking both the volumetric average of the Smagorinsky viscosity as well as the largest time mean value that was observed anywhere in the model domain. Use of either value resulted in a numerically unstable simulation. This experience illustrates that numerical stability requires a constant biharmonic viscosity that is able to control the largest deformation rates that occur at any place *and time*. Consequently, the time mean Smagorinsky biharmonic viscosity may be everywhere less than the required constant coefficient biharmonic viscosity! Further experimentation found that a constant viscosity of 2×10^{10} m^4 s^{-1} gave a numerically stable simulation.

The flow has slightly (3%) less kinetic energy and available potential energy averaged over 1000 days with the constant biharmonic viscosity than with the Smagorinsky viscosity. However, the two cases are qualitatively similar, and the difference is not statistically significant. This is reassuring, since there is a long tradition of using a constant coefficient biharmonic vis-
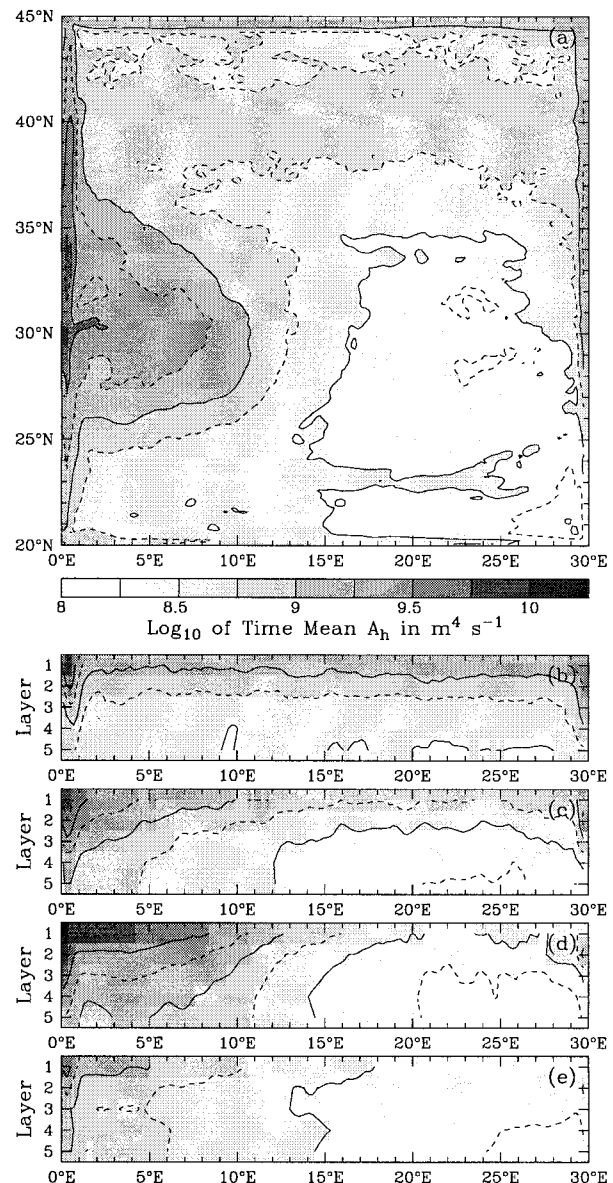
FIG. 2. Log$_{10}$ of the time-averaged biharmonic Smagorinsky viscosity (m^4 s^{-1}) over 1000 days in a five-layer HIM simulation of two wind-driven gyres. (a) A plan view of the second layer from the top. (b), (c), (d), and (e) Cross sections at 40°, 35°, 30°, and 25°N, respectively. The viscosity (and horizontal deformation rate) in the eddy-rich western boundary current region is almost two orders of magnitude larger than in the quiescent abyssal shadow region (Luyten et al. 1983) in the southeast corner of the basin. The slightly enhanced values near the boundaries in the south, east, and north are associated with boundary currents. The equivalent instantaneous fields are much less smooth than these time averages.

cosity in eddy-permitting ocean model simulations. In these simulations, the turbulence and the eddy kinetic energy are dominated by the western boundary region. The differences between simulations using constant-coefficient and Smagorinsky biharmonic viscosities will be more pronounced when those simulations include multiple, independent turbulent regimes such as for the
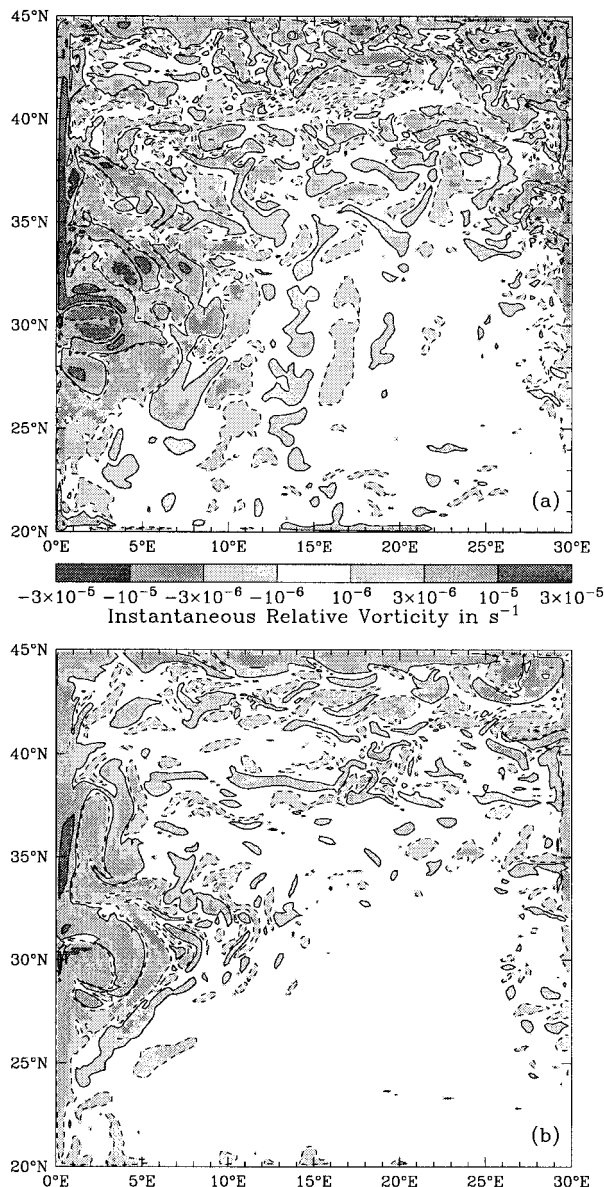
FIG. 3. Instantaneous relative vorticity of the second layer in five-layer HIM simulations of two wind-driven gyres using (a) the biharmonic Smagorinsky scheme and (b) Laplacian Smagorinsky scheme. Note the enhanced level of activity with the biharmonic scheme.

World Ocean. Also, it should be reemphasized that the appropriate value of the constant coefficient viscosity was only known after actually running several simulations. The Smagorinsky viscosity avoids the need for an a priori guess at this value.

As with the thermally driven channel, a Laplacian Smagorinsky scheme substantially suppresses the eddies relative to the biharmonic Smagorinsky scheme, as is readily seen by comparing instantaneous relative vorticities of an interior layer (Fig. 3). The eddy kinetic energy averaged over 1000 days is smaller by a factor of 4 with the Laplacian Smagorinsky scheme compared with the biharmonic Smagorinsky scheme, relative to the total kinetic energy and available potential energy of each simulation. The kinetic energy of the mean flow is reduced by less than 20% with the Laplacian, while the available potential energy is slightly (3%) larger with the Laplacian compared with the biharmonic. The difference in the levels of eddy activity between these simulations is due to suppression of the eddies by the Laplacian, not to a change in the baroclinic instability of the mean flow.

A simulation with half the resolution, but using the same nondimensional coefficient with the Smagorinsky biharmonic viscosity, gave perfectly sensible results; that is, the admitted scales remained resolved. The same would not occur with a constant coefficient biharmonic viscosity, which generally requires that the viscosity be increased as the resolution decreases. This illustrates the very convenient property of the Smagorinsky biharmonic scheme: only a single nondimensional coefficient needs to be set, and this coefficient is independent of resolution, so long as the same physical regime is present. It is only a function of the model's numerics.

The CPU time required for the simulation with the Smagorinsky biharmonic scheme was only 3% more than with the constant coefficient biharmonic scheme and 4% more than with the Smagorinsky Laplacian scheme. Note that this difference is for a model without thermodynamics. For more realistic models, the relative cost of the scheme would be even less.

6. Summary and conclusions

This paper argues for the utility of a Smagorinsky-like viscosity for use with a biharmonic friction operator as a numerical closure scheme for eddy-permitting large-scale ocean models. This proposal is natural for one aiming to simulate geostrophic eddies in a realistic inhomogeneous environment such as the World Ocean. That is, the biharmonic operator, being more scale selective than the Laplacian operator, acts less on the large scales of motion, which are of direct interest and are better resolved, than the small scales, where enstrophy cascades. As an example of this scale selectivity, we ran a thermally forced channel that showed that the Laplacian operator, even when using a Smagorinsky viscosity, can unnecessarily suppress physically unstable modes that are well resolved by the model grid.

The utility of the Smagorinsky approach to determining viscosity follows from its providing a local deformation rate and grid-size-dependent viscosity that naturally adapts to the inhomogeneities present in realistic ocean simulations. An eddy-permitting sector model provided a vivid illustration of the ability of the Smagorinsky scheme to maintain the high levels of viscosity in the western boundary current, needed for numerical stability reasons, while allowing much lower levels in the more quiescent interior. In contrast, ex-

periments run with constant biharmonic viscosities either underdissipated the flow, and tended to go numerically unstable, or dissipated the flow more than with the Smagorinsky scheme.

Ideally, the beneficial properties of the Smagorinsky scheme are realized by setting a single nondimensional constant. Sector experiments with different horizontal resolutions illustrated that the *same* value of this constant is appropriate regardless of the resolution, so long as similar physical features are present. Consequently, the Smagorinsky scheme effectively reduces the number of parameters that must be tuned when designing a new experiment. This aspect of the scheme can be quite important especially for large-scale eddy-permitting models. In practice, one should be aware of the need to resolve boundary currents, especially where the flow is less vigorous, since the Smagorinsky viscosity might be too small in these regions. This issue is more relevant for coarse models, but in general it may be necessary to set a minimum allowable viscosity determined by the relevant flow-independent frictional boundary layer scaling.

The biharmonic Smagorinsky scheme has little physical justification for large-scale geophysical simulations. Indeed, for that matter, neither does the more traditional Laplacian scheme. Yet, as argued here, the biharmonic scheme is an ideal numerical closure to which a physically based parameterization of the effects of unresolved scales may be added, if necessary. Assuming that the physical parameterization involves some form of a Laplacian, the enhanced scale selectivity of the biharmonic operator guarantees that at sufficiently large scales, the effects of resolved fluctuations and the physical subgrid parameterization will dominate the simulation, and the numerically based Smagorinsky biharmonic closure will be negligible.

On a Cray T90, the Smagorinsky scheme in our idealized examples required roughly 2%–4% more for the total model runtime relative to a constant horizontal viscosity. When using a biharmonic operator, the models ran some 5%–10% slower than with the Laplacian. In either case, the added cost should be gauged against the cost necessary to increase the grid resolution enough to admit comparably rich geostrophic eddy activity with the Laplacian operator and/or a constant viscosity. From this perspective, the biharmonic Smagorinsky scheme is very economical.

APPENDIX
The Friction Operators

We present here the Laplacian and biharmonic friction operators applicable for any set of orthogonal curvilin-

ear coordinates in the transverse directions, as well as methods used for their discretization. As generalized orthogonal coordinates are commonly used by ocean models, such as those of Blumberg and Mellor (1987), Haidvogel et al. (1991), Smith et al. (1995), Madec and Imbard (1996), and Murray and Reason (1999, manuscript submitted to *J. Comput. Phys.,* hereafter MR), it is important to provide methods for implementing the ideas described in the main text in such a framework. Mathematical details are largely omitted in the following, as they can be found in the classical literature, such as Aris (1962) and Batchelor (1967). The papers by Williams (1972), Smagorinsky (1993), Wajsowicz (1993), Sadourny and Maynard (1997), Pacanowski and Griffies (1999), and MR also provide discussions directly relevant to the following.

We follow the general tensorial notation of Aris (1962) as it represents a simple and powerful generalization of the more familiar Cartesian tensor notation. In particular, the summation convention is employed, in which repeated indices are summed. Additionally, partial derivatives are prefaced by a comma, and covariant derivatives by a semicolon.

a. Coordinate assumptions

For the transverse or "horizontal" coordinates (those within the surface of the sphere), we restrict attention to coordinates that are locally orthogonal and that do not depend on the vertical position. As such, the squared infinitesimal distance between two points in a shallow ocean takes the form

$$(ds)^2 = (h_1 \, dx^1)^2 + (h_2 \, dx^2)^2 + (dz)^2$$
$$= (dx)^2 + (dy)^2 + (dz)^2. \tag{A1}$$

In this expression, $g_{11} = (h_1)^2$ and $g_{22} = (h_2)^2$ are nonnegative metric components, each dependent on the two transverse coordinates (x^1, x^2). The familiar case of spherical coordinates $(x^1, x^2) = (\lambda, \phi)$ leads to $(h_1)^2 = R^2 \cos^2\phi$ and $(h_2)^2 = R^2$, with λ the longitude and ϕ the latitude. The coordinate increments $dx = h_1 \, dx^1$ and $dy = h_2 \, dy^1$ represent the infinitesimal physical distance in the two generalized transverse directions.

b. Laplacian friction

We rely on Williams (1972), Smagorinsky (1993), and Wajsowicz (1993) to detail the assumptions leading up to the form of the Laplacian friction operator. For present purposes, we start by assuming that the frictional stress tensor can be split into vertical and horizontal (or transverse) subtensors. Focusing on the 2×2 transverse stress tensor, we note that this tensor is proportional to the strain arising from horizontal deformations in the fluid (summarized by the transverse strain tensor), it is symmetric (which is required for the conservation of angular momentum), trace free, and possesses axial

symmetry about the local vertical (which arises from transverse isotropy). These assumptions lead to the transverse frictional stress tensor

$$\tau^{ab} = \rho A (2 e^{ab} - g^{ab} e^c_c), \tag{A2}$$

where A is a nonnegative kinematic viscosity with dimensions length^2 time^{-1}, ρ is the fluid density, and the tensor labels $a, b = 1, 2$ represent the horizontal directions. The symmetric transverse strain tensor e_{ab} takes the form $2 e_{ab} = u_{a;b} + u_{b;a}$. The direct relation between strain, which is a kinematic property of the fluid, and stress, which leads to dynamical response through Newton's law, can be considered a general statement of Hooke's law. We note that the transverse isotropy assumption has been dropped by Large et al. (2000) which leads to two kinematic viscosities for the transverse stress tensor. More conventional treatments of friction in ocean models follow the approach given here.

The covariant divergence of the frictional stress tensor (19) yields the frictional force vector per unit volume $\rho F^m = \tau^{mn}_{;n}$, which acts on a parcel of fluid. Performing this divergence leads to the physical friction components $(F^x, F^y) = (h_1 F^1, h_2 F^2)$:

$$\rho F^x = g^{-1}_{22} (g_{22} \rho A D_T)_{,x} + g^{-1}_{11} (g_{11} \rho A D_S)_{,y} \quad \text{and} \tag{A3}$$

$$\rho F^y = g^{-1}_{22} (g_{22} \rho A D_S)_{,x} - g^{-1}_{11} (g_{11} \rho A D_T)_{,y}. \tag{A4}$$

Introduced here are the *horizontal tension*

$$D_T = h_2 (u/h_2)_{,x} - h_1 (v/h_1)_{,y} \tag{A5}$$

and *horizontal shearing strain*

$$D_S = h_1 (u/h_1)_{,y} + h_2 (v/h_2)_{,x}, \tag{A6}$$

where $(u, v) = (h_1 Dx^1/Dt, h_2 Dx^1/Dt)$ are the physical velocity components (e.g., in spherical coordinates, $(u, v) = R(\cos\phi D\lambda/Dt, D\phi/Dt)$). Both D_T and D_S have physical dimensions of inverse time, and together they quantify the rate of horizontal deformation experienced by a fluid parcel. The spherical coordinate version of these expressions are given by Smagorinsky (1963, 1993).

c. Biharmonic friction

To derive the biharmonic friction operator, we iterate twice on the Laplacian, where each step uses the square root of the biharmonic viscosity. Specifically, the components $\tilde{F}^a$ of the biharmonic friction vector are derived from $\rho \tilde{F}^a = \Theta^{ab}_{;b}$, where $\Theta^{ab} = -\rho\sqrt{B}(2 E^{ab} - g^{ab} E^c_c)$ is a symmetric "stress" tensor. The components of the symmetric "strain" tensor are given by $2 E^{ab} = F^{a;b} + F^{b;a}$. Here, F^a is the frictional force per unit mass determined through the second-order frictional stress tensor $\rho F^a = \tau^{ab}_{;b}$ as derived in the previous subsection, but with $\sqrt{B}$ used as the viscosity when computing τ^{ab}. Notably, as with Laplacian friction, since the biharmonic friction arises from the covariant divergence of

a symmetric tensor, it will not impart internal sources or sinks of angular momentum.

d. Effects on kinetic energy

The horizontal kinetic energy of a fluid parcel is given by $2K = \rho\, dV\, g_{ab} u^a u^b$, and its evolution under the effects from transverse friction is $\dot{K} = dV\, g_{ab} u^a \rho \tau^{bn}_{;n}$. For Laplacian friction, integration over a domain and neglect of the surface terms leads to the contribution

$$\int \dot{K} = -\int dV\, \rho A (D_T^2 + D_S^2), \tag{A7}$$

which is negative semidefinite so long as the horizontal viscosity is nonnegative. In Cartesian coordinates, this contribution can be put in the familiar form $-\int dV\, \rho A(|\nabla u|^2 + |\nabla v|^2)$. The scalar quantity

$$|D|^2 = D_T^2 + D_S^2 = (2\rho^2 A^2)^{-1} \tau^{ab} \tau_{ab} \tag{A8}$$

represents the total squared horizontal deformation rate of a fluid parcel. It is independent of the choice of horizontal coordinates. As mentioned in section 3, $|D|$ is used for defining the timescale when computing the Smagorinsky viscosity.

For horizontal biharmonic friction, similar manipulations, in which all boundary contributions are neglected, lead to the contribution

$$\int \dot{K} = -\int dV\, \rho F_m F^m, \tag{A9}$$

which is also nonpositive. In Cartesian coordinates, this result can be put in the form $-\int dV\, \rho\{[\nabla \cdot (\sqrt{B}\nabla u)]^2 + [\nabla \cdot (\sqrt{B}\nabla v)]^2\}$. The Cartesian form exposes the need to use $\sqrt{B}$ in order to dissipate kinetic energy. Alternatives, such as $\nabla \cdot (B\nabla \cdot \nabla^2 \psi)$ or $\nabla^2(\nabla \cdot B\nabla \psi)$ generally dissipate kinetic energy only when B is spatially constant, and so are not considered here when using the Smagorinsky viscosity.

e. Generalized vertical coordinates

Fundamental to the earlier derivations is the special nature of the local vertical direction $\hat{z}$, which is parallel to gravity. The nonorthogonal generalized vertical coordinate systems employed in ocean models also maintain the special nature of the vertical, hence allowing for the 2 × 2 transverse stress tensor to be isolated. Consequently, the only transformation that must be performed is one that converts the divergence of the stress tensor into the (x, y, σ) coordinates, so that we can identify the appropriate forms of the friction vector components. In particular, we simply need to transform the horizontal partial derivatives from constant z surfaces to constant σ surfaces. For the zonal friction, this derivation leads to

$$z_{,\sigma}\rho F^x = g_{22}^{-1}(z_{,\sigma}g_{22}\rho AD_T)_{,x} + g_{11}^{-1}(z_{,\sigma}g_{11}\rho AD_S)_{,y}$$
$$- (z_{,x}\rho AD_T)_{,\sigma} - (z_{,y}\rho AD_S)_{,\sigma}, \quad \text{(A10)}$$

where the horizontal derivatives are now taken along constant σ surfaces. The nonorthogonal transformation between (x, y, z) and (x, y, σ) is nonsingular so long as the Jacobian $\partial z/\partial\sigma = z_{,\sigma}$, also called the specific thickness, is of one sign. We assume this to be the case. The dimensionless vector $(z_{,x}, z_{,y}, 0)$, where derivatives are taken with σ constant, measures the slope of the σ surfaces relative to z surfaces. Assuming that this slope is small leads to the friction components

$$z_{,\sigma}\rho F^x = g_{22}^{-1}(z_{,\sigma}g_{22}\rho AD_T)_{,x} + g_{11}^{-1}(z_{,\sigma}g_{11}\rho AD_S)_{,y} \quad \text{(A11)}$$

and

$$z_{,\sigma}\rho F^y = g_{22}^{-1}(z_{,\sigma}g_{22}\rho AD_S)_{,x} - g_{11}^{-1}(z_{,\sigma}g_{11}\rho AD_T)_{,y}. \quad \text{(A12)}$$

Consequently, the only practical difference from the geopotential model is the presence of the specific thickness factor $z_{,\sigma}$. This factor ensures a proper momentum balance for the layer-integrated equations of motion. Furthermore, motivated by simplicity and momentum balance, we prescribe that thickness appears only when computing the second part of the biharmonic operator.

f. Discretization methods

On a C grid, the horizontal strain D_S [Eq. (A6)] is naturally defined at the vorticity point, and the horizontal tension D_T [Eq. (A5)] is defined at the thickness point. These positions are ideal for then constructing the zonal and meridional friction components through the spatial derivatives given in Eqs. (A3) and (A4). Boundaries are handled with no-normal flow/free slip, which means D_S vanishes on all boundaries. The analogous boundary conditions are applied when constructing the biharmonic operator. This discretization has no computational modes.

A common starting point for discretizing friction in B-grid ocean models is the "Laplacian plus metric" form of the friction operator detailed by Bryan (1969), Wajsowicz (1993), and MR, in contrast to the form exposing the rates of deformation given by Eqs. (A3) and (A4). The Laplacian plus metric form manipulates the friction operator into a scalar Laplacian operator acting on the velocity components, plus added "frictional metric terms." This approach, however, does not utilize the deformation rate calculation, needed for the Smagorinsky viscosity, for a calculation of the friction operator. Additionally, the computation of frictional metric terms is cumbersome and generally leads to computational modes. As a result, we have considered the following alternative approach based on exploiting the self-adjointness of the frictional operator.

The key idea is to note that the negative semidefinite kinetic energy dissipation

$$S = -\int dV\, \rho A(D_T^2 + D_S^2), \quad \text{(A13)}$$

which is a functional of the velocity field and its spatial gradients, has a functional derivative given by

$$\frac{1}{2\rho}\frac{\delta S}{\delta u^a} = g_{ab}F^b. \quad \text{(A14)}$$

To obtain this result, we assumed the viscosity is independent of the flow. This assumption amounts to assuming a linear friction operator. We exploit this result to derive a discretization of the linear friction operator and then extend it to the case of the Smagorinsky nonlinear viscosity. A similar approach was used for the isoneutral diffusion operator, which is a nonlinear form of diffusion when acting on the temperature and salinity fields (see Griffies et al. 1998 for more details).

Upon recognizing the functional relation (A14), the approach is to discretize the kinetic energy dissipation S and then to perform the discrete functional derivative. The result is the physical components of the discretized friction vector given by

$$F_{i,j}^x = \frac{1}{2\rho(h_1)_{i,j}V_{i,j}^U}\frac{\partial S}{\partial(u^1)_{i,j}} \quad \text{and} \quad \text{(A15)}$$

$$F_{i,j}^y = \frac{1}{2\rho(h_2)_{i,j}V_{i,j}^U}\frac{\partial S}{\partial(u^2)_{i,j}}, \quad \text{(A16)}$$

where the subscripts i, j denote discrete model lattice points. For a Bousinnesq fluid, as assumed for MOM, ρ is replaced by ρ_o. Note that the volume of the velocity cell V^U accounts for the difference between a dimensionless Kronecker delta function used in the discrete case, and the Dirac delta function, whose dimensions are inverse volume, used to derive the continuum expression (A14).

Details of this discretization are analogous to the isoneutral diffusion operator discretization. Griffies et al. (1998) and Pacanowski and Griffies (1999) documents these details, and so they are not repeated here. Notably, the friction operator's stencil comprises weighted triads of velocity points analogous to the tracer/density triads present in the isoneutral diffusion operator. Boundaries are handled using no-slip conditions for both the Laplacian and biharmonic operators. The result is a discrete B-grid friction operator that has no computational modes, is guaranteed to dissipate kinetic energy, exploits the calculation of the deformation rates for both the Smagorinsky viscosity and the stress tensor, and generalizes naturally to arbitrary orthogonal coordinates.

REFERENCES

Aris, R., 1962: *Vectors, Tensors and the Basic Equations of Fluid Mechanics.* Dover, 286 pp.
Batchelor, G. K., 1967: *An Introduction to Fluid Dynamics.* Cambridge University Press, 615 pp.
Bleck, R., and D. B. Boudra, 1981: Initial testing of a numerical ocean circulation model using a hybrid- (quasi-isopycnic) vertical coordinate. *J. Phys. Oceanogr.,* **11,** 755–770.
——, C. Rooth, D. Hu, and L. T. Smith, 1992: Salinity-driven ther-

mocline transients in a wind and thermohaline forced isopycnic coordinate model of the North Atlantic. *J. Phys. Oceanogr.,* **22,** 1486–1505.

Blumberg, A. F., and G. L. Mellor, 1987: A description of a three-dimensional coastal ocean circulation model. *Three-Dimensional Coastal Ocean Models,* N. Heaps, Ed., Vol. 4, Amer. Geophys. Union, 1–16.

Boer, G. J., and T. G. Shepherd, 1983: Large-scale two-dimensional turbulence in the atmosphere. *J. Atmos. Sci.,* **40,** 164–184.

Böning, C. W., and R. G. Budich, 1992: Eddy dynamics in a primitive equation model: Sensitivity to horizontal resolution and friction. *J. Phys. Oceanogr.,* **22,** 361–381.

Bryan, K., 1969: A numerical method for the study of the circulation of the world ocean. *J. Comput. Phys.,* **4,** 347–376.

——, S. Manabe, and R. C. Pacanowski, 1975: A global ocean-atmosphere climate model. Part II. The oceanic circulation. *J. Phys. Oceanogr.,* **5,** 30–46.

Galperin, B., and S. A. Orszag, 1993: *Large Eddy Simulation of Complex Engineering and Geophysical Flows.* Cambridge University Press, 600 pp.

Gill, A. E., 1982: *Atmosphere–Ocean Dynamics.* Academic Press, 662 pp.

Gille, S. T., 1997: The southern ocean momentum balance: Evidence for topographic effects from numerical model output and altimeter data. *J. Phys. Oceanogr.,* **27,** 2219–2232.

Griffies, S. M., A. Gnanadesikan, R. C. Pacanowski, V. Larichev, J. K. Dukowicz, and R. D. Smith, 1998: Isoneutral diffusion in a *z*-coordinate ocean model. *J. Phys. Oceanogr.,* **28,** 805–830.

——, R. C. Pacanowski, and R. W. Hallberg, 2000: Spurious diapycnal mixing associated with advection in a *z*-coordinate ocean model. *Mon. Wea. Rev.,* **128,** 538–564.

Haidvogel, D. B., J. L. Wilkin, and R. Young, 1991: A semi-spectral primitive equation ocean circulation model using vertical sigma and orthogonal curvilinear horizontal coordinates. *J. Comput. Phys.,* **94,** 151–185.

Hallberg, R., 1995: Some aspects of the circulation in ocean basins with isopycnals intersecting the sloping boundaries. Ph.D thesis, University of Washington, 244 pp. [Available from Dept. of Oceanography, University of Washington, Seattle, WA.]

Haltiner, G. J., and R. T. Williams, 1980: *Numerical Prediction and Dynamic Meteorology.* Wiley, 477 pp.

Held, I. M., R. T. Pierrehumbert, S. T. Garner, and K. L. Swanson, 1995: Surface quasi-geostrophic dynamics. *J. Fluid Mech.,* **282,** 1–20.

Holland, W. R., 1978: The role of mesoscale eddies in the general circulation of the ocean—Numerical experiments using a wind-driven quasi-geostrophic model. *J. Phys. Oceanogr.,* **8,** 363–392.

——, J. C. Chow, and F. O. Bryan, 1998: Application of a third-order upwind scheme in the NCAR ocean model. *J. Climate,* **11,** 1487–1493.

Kazantsev, E., J. Sommeria, and J. Verron, 1998: Subgrid-scale eddy parameterization by statistical mechanics in a barotropic ocean model. *J. Phys. Oceanogr.,* **28,** 1017–1042.

Large, W. K., G. Danabasoglu, J. C. McWilliams, P. R. Gent, and F.

O. Bryan, 2000: Equatorial circulation of a global ocean climate model with anisotropic horizontal viscosity. *J. Phys. Oceanogr.,* in press.

Leith, C. E., 1968: Diffusion approximation for two-dimensional turbulence. *Phys. Fluids,* **10,** 1409–1416.

Leith, C. E. 1996: Stochastic models of chaotic systems. *Physica D,* **98,** 481–491.

Leonard, B. P., 1979: A stable and accurate convective modelling procedure based on quadratic upstream interpolation. *Comput. Methods Appl. Mech. Eng.,* **19,** 59–98.

Luyten, J. R., J. Pedlosky, and H. Stommel, 1983: The ventilated thermocline. *J. Phys. Oceanogr.,* **13,** 292–309.

Madec, G., and M. Imbard, 1996: A global ocean mesh to overcome the North Pole singularity. *Climate Dyn.,* **12,** 381–388.

Munk, W. H., 1950: On the wind-driven ocean circulation. *J. Meteor.,* **7,** 3–29.

Pacanowski, R. C., and S. M. Griffies, 1999: The MOM 3 manual. Geophysical Fluid Dynamics Laboratory Tech. Rep., Princeton, NJ, 680 pp. [Available online via anonymous ftp from GFDL.gov.]

Rhines, P. B., 1977: The dynamics of unsteady currents. *The Sea,* E. D. Goldberg et al., Eds., Vol. 6, Wiley-Interscience, 189–318.

Rosati, A., and K. Miyakoda, 1988: A general circulation model for upper ocean simulation. *J. Phys. Oceanogr.,* **18,** 1601–1626.

Sadourny, R., and C. Basdevant, 1985: Parameterization of subgrid scale barotropic and baroclinic eddies in quasi-geostrophic models: Anticipated potential vorticity method. *J. Atmos. Sci.,* **42,** 1353–1363.

——, and K. Maynard, 1997: Formulations of lateral diffusion in geophysical fluid dynamics models. *Numerical Methods in Atmospheric and Oceanic Modelling,* C. A. Lin, R. Laprise, and H. Ritchie, Eds., NRC Research Press, 547–556.

Salmon, R., 1998: *Lectures on Geophysical Fluid Dynamics.* Oxford University Press, 378 pp.

Semtner, A. J., and Y. Mintz, 1977: Numerical simulation of the Gulf Stream and mid-ocean eddies. *J. Phys. Oceanogr.,* **7,** 208–230.

Smagorinsky, J., 1963: General circulation experiments with the primitive equations: I. The basic experiment. *Mon. Wea. Rev.,* **91,** 99–164.

Smagorinsky, J., 1993: Some historical remarks on the use of non-linear viscosities. *Large Eddy Simulation of Complex Engineering and Geophysical Flows,* B. Galperin and S. A. Orszag, Eds., Cambridge University Press, 3–36.

Smith, R. D., S. Kortas, and B. Meltz, 1995: Curvilinear coordinates for global ocean models. Los Alamos Rep. LA-UR-95-1146, 52 pp. [Available from Los Alamos National Laboratory, Group T-3, Los Alamos, N.M. 87545.]

——, M. E. Maltrud, F. O. Bryan, and M. W. Hecht, 2000: Numerical simulation of the North Atlantic Ocean at $\frac{1}{10}°$. *J. Phys. Oceanogr.,* **30,** 1532–1561.

Wajsowicz, R. C., 1993: A consistent formulation of the anisotropic stress tensor for use in models of the large-scale ocean circulation. *J. Comput. Phys.,* **105,** 333–338.

Williams, G. P., 1972: Friction term formulation and convective instability in a shallow atmosphere. *J. Atmos. Sci.,* **29,** 870–876.